Journal of Cellular Physiology

Interactions Between Integrin Ligand Density and Cytoskeletal Integrity Regulate BMSC Chondrogenesis

JOHN T. CONNELLY,[1] ANDRÉS J. GARCÍA,[1] AND MARC E. LEVENSTON[1,2]*

[1]George W. Woodruff School of Mechanical Engineering, Georgia Institute of Technology, Atlanta, Georgia

[2]Department of Mechanical Engineering, Stanford University, Stanford, California

Interactions with the extracellular matrix play important roles in regulating the phenotype and activity of differentiated articular chondrocytes; however, the influences of integrin-mediated adhesion on the chondrogenesis of mesenchymal progenitors remain unclear. In the present study, agarose hydrogels were modified with synthetic peptides containing the arginine-glycine-aspartic acid (RGD) motif to investigate the effects of integrin-mediated adhesion and cytoskeletal organization on the chondrogenesis of bone marrow stromal cells (BMSCs) within a three-dimensional culture environment. Interactions with the RGD-modified hydrogels promoted BMSC spreading in a density-dependent manner and involved αvβ3 integrin receptors. When cultured with the chondrogenic supplements, TGF-β1 and dexamethasone, adhesion to the RGD sequence inhibited the stimulation of sulfated-glycosaminoglycan (sGAG) production in a RGD density-dependent manner, and this inhibition could be blocked by disrupting the F-actin cytoskeleton with cytochalasin D. In addition, interactions with the RGD-modified gels promoted cell migration and aggrecanase-mediated release of sGAG to the media. While adhesion to the RGD sequence inhibited BMSC chondrogenesis in the presence of TGF-β1 and dexamethasone, osteocalcin and collagen I gene expression and alkaline phosphatase activity were enhanced by RGD interactions in the presence of serum-supplemented medium. Overall, the results of this study demonstrate that integrin-mediated adhesion within a three-dimensional environment inhibits BMSC chondrogenesis through actin cytoskeleton interactions. Furthermore, the effects of RGD-adhesion on mesenchymal differentiation are lineage-specific and depend on the biochemical composition of the cellular microenvironment.

J. Cell. Physiol. 217: 145–154, 2008.

Cell shape is closely linked to the phenotype of mature articular chondrocytes, which display primarily rounded morphologies in vivo. During in vitro monolayer culture however, chondrocytes readily adhere to and spread on surfaces. These changes in morphology are associated with a gradual loss of collagen type II and proteoglycan synthesis (von der Mark et al., 1977). Disruption of the F-actin cytoskeleton with cytochalasin D inhibits this dedifferentiation process (Newman and Watt, 1988), while culturing chondrocytes within three-dimensional hydrogels preserves their rounded morphology and chondrocytic phenotype (Kolettas et al., 1995). Although cell morphology is an important regulator of the mature chondrocyte, the role of cytoskeletal organization in the chondrogenesis of mesenchymal progenitors is less clear. The use of chemical inhibitors to block actin polymerization or actin-myosin contractility has yielded differing results depending on the cell types and culture conditions examined (Lim et al., 2000; Woods et al., 2005; Woods and Beier, 2006), suggesting that cell morphology and cytoskeletal organization play complex and regulated roles in the process of chondrogenesis.

Integrin-mediated adhesion to the extracellular matrix provides cell anchorage and a direct link between the F-actin cytoskeleton and the surrounding environment. Upon binding to their ligands, integrin receptors cluster and form supramolecular structures termed focal complexes (Calderwood et al., 1999; Maheshwari et al., 2000), which directly connect to F-actin filaments through scaffolding proteins such as vinculin and talin (Critchley, 2004). In this manner, cell adhesion to the ECM can direct the formation of actin stress fibers and influence the overall organization of the cytoskeleton. In addition, kinases and other signaling molecules, such as focal adhesion kinase (FAK) and src can associate with focal complexes and provide a mechanism for transducing signals from the cell's extracellular environment (Giancotti and Ruoslahti, 1999; Critchley, 2004). Cytoskeletal dynamics are regulated by the family of small Rho GTPases including RhoA, Rac-1, and cdc42 (Nobes and Hall, 1995). Rho kinase (ROCK) is one of RhoAs effectors and is responsible for myosin light chain (MLC) phosphorylation and actin-myosin contractility (Amano et al., 1996; Leung et al., 1996). The RhoA/ROCK signaling pathway mediates multiple cellular activities including migration (Ai et al., 2001), proliferation (Iwamoto et al., 2000), and differentiation (McBeath et al., 2004), and can influence the response to growth factors (Kaartinen et al., 2002) and integrin-based adhesion (Imamura et al., 2000).

Cell morphology is an important regulator of differentiation for multiple cell types. Recently, the role of cytoskeletal organization in mesenchymal lineage selection was examined using micropatterned surfaces and inhibitors of RhoA/ROCK signaling (McBeath et al., 2004). In this report, cell adhesion and spreading stimulated osteogenesis through RhoA activation of ROCK, while more rounded cell morphologies enhanced adipocyte differentiation via RhoA inactivation. Although these results indicate that cytoskeletal organization is a key factor in mesenchymal stem cell differentiation, its influence on chondrogenesis remains unclear. Several studies have reported

Contract grant sponsor: National Science Foundation (NSF);
Contract grant number: EEC 9731643.

*Correspondence to: Marc E. Levenston, 233 Durand Building, Stanford University, Stanford, CA 94305-4038.
E-mail: levenston@stanford.edu

Received 13 February 2008; Accepted 24 March 2008

DOI: 10.1002/jcp.21484

enhanced chondrogenesis in chick limb bud cells by disrupting F-actin polymerization during monolayer culture (Lim et al., 2000). In contrast, the application of cytochalasin D or the ROCK inhibitor (Y-27632) to micromass cultures of ATDC or mouse limb bud cells inhibited the expression of collagen II and aggrecan genes (Woods and Beier, 2006). Taken together, these reports suggest that the influence of cytoskeletal organization on chondrogenesis may depend on the degree of cell spreading and involve additional signals from the surrounding microenvironment.

Previous studies in our laboratory have shown that integrin-mediated adhesion to RGD-modified alginate inhibits the chondrogenesis of BMSCs (Connelly et al., 2007). Given the direct connection between integrin receptors and the actin cytoskeleton, adhesion to the ECM could regulate the differentiation of mesenchymal progenitors by modulating the degree of cytoskeletal organization. Therefore, the objective of this study was to investigate the effects of interactions between integrin-mediated adhesion and cytoskeletal organization on the chondrogenesis of BMSCs within a 3D environment. In these experiments, RGD peptides were conjugated to agarose hydrogels, and integrin-mediated adhesion to the RGD motif promoted BMSC spreading in a density dependent manner. This system allowed for the controlled presentation of specific adhesive ligands and varying degrees of cytoskeletal organization. The influence of these defined cell–matrix interactions on the chondrogenic response of BMSCs to TGF-β1 and dexamethasone was examined over a range of RGD densities and in the presence of the cytoskeleton inhibitors cytochalasin D and Y-27632. Furthermore, the specificity of these responses to chondrogenesis was evaluated by investigating the BMSC response to serum supplemented medium within the same modified agarose gels.

Materials and Methods

Materials

The synthetic peptides GRGESP and GRGDSP were from Bachem (King of Prussia, PA), and the sulfo-SANPAH cross-linker was from Pierce (Rockford, IL). Seaprep agarose was from Cambrex (Frederick, MD). Immature bovine hind limbs were from Research 87 (Marlborough, MA). Recombinant human TGF-β1 was from R&D Systems (Minneapolis, MN), and basic-fibroblast growth factor (bFGF) was from Peprotech (Rocky Hill, NJ). Cytochalasin D and Y-26732 were from Calbiochem (San Diego, CA). The WST-1 assay kit was from BioVision (Mountain View, CA). The functional blocking antibody against the β1 integrin (AIIB2) was from the University of Iowa Developmental Studies Hybridoma Bank (Iowa City, IA), and the anti-αvβ3 antibody (LM609) was from Chemicon (Temecula, CA). The mouse IgG isotype control was from Jackson Immunological Research (West Grove, PA). The anti-vinculin antibody was from Sigma–Aldrich (St. Louis, MO), and the FITC anti-mouse antibody was from Abcam (Cambridge, MA). The anti-NITEGE antibody JSCNIT was generously provided by John Sandy Ph.D. (Rush University, Chicago, IL). AlexaFluor594-conjugated phalloidin, AlexaFluor488-conjugated anti-rabbit IgG, and the Live/Dead staining kit were from Molecular Probes (Eugene, OR).

Preparation of RGD-modified agarose

The synthetic peptides GRGESP and GRGDSP were conjugated to agarose hydrogels with the heterobifunctional sulfo-SANPAH cross-linker according to a modified, published protocol (Dodla and Bellamkonda, 2006). The primary amines on the peptides were reacted with the NHS-ester group of the sulfo-SANPAH at room temperature for 4 h in the dark with a 10-fold molar excess of the cross-linker. Seaprep agarose solutions were prepared in Ca^{++}/Mg^{++}-free PBS, autoclaved, and cooled to 37°C. One part peptide/sulfo-SANPAH solution was combined with three parts 4% agarose and mixed thoroughly to yield a 3% agarose gel construct. The mixture was exposed to 365 nm UV light for 3 min to activate the photoreactive groups of the sulfo-SANPAH and conjugate the peptide to free CH-groups in the agarose. The agarose was allowed to gel at 4°C for 20 min and washed multiple times with PBS to remove the unbound peptide and cross-linker. Tethered peptide densities were determined by fluorescence detection of a biotinylated peptide following agarase digestion and blotting onto nitrocellulose. The conjugation efficiency was approximately 25% of the initial concentration over the range of densities examined in this study.

Cell seeding and gel culture

Bone marrow was harvested from the tibiae and femora of an immature calf as previously described (Connelly et al., 2007). The adherent BMSCs were expanded three times in low glucose Dulbecco's Modified Eagles Medium supplemented with 10% fetal bovine serum and 1 ng/ml basic-FGF. The 3% modified agarose gels were melted at 45°C and cooled to 37°C. BMSCs were then seeded into cylindrical (4 mm diameter) gels by resuspending the cells in the melted agarose at a density of 10^7 cells/ml and casting the cell suspension into custom molds. The gels were cooled at 4°C for 30 min and transferred to fresh culture medium. The basal, chemically defined medium consisted of high glucose DMEM, 1% ITS+ Premix, 1% NEAA, 1% antibiotic/antimycotic, and 50 μg/ml ascorbate, and the chondrogenic medium was supplemented with 10 ng/ml TGF-β1 and 100 nM dexamethasone. For the integrin blocking experiments, BMSCs were incubated with 20 μg/ml of anti-αvβ3, anti-β1, or mouse IgG for 20 min in DMEM prior to seeding into agarose, and the gels were cultured overnight in chondrogenic medium with 20 μg/ml of the same antibodies (Connelly et al., 2007). In some experiments, the chondrogenic medium was further supplemented with 10 μM Y-27632, 0.3 μM cytochalasin D, or the carrier alone (0.01% DMSO). The fetal bovine serum (FBS)-supplemented medium consisted of DMEM, 10% FBS, NEAA, antibiotic/antimycotic, and ascorbate. BMSC seeded gels were cultured up to 8 days under the specified conditions and media were collected and changed every 2 days.

Fluorescence imaging and analysis

Agarose gels were fixed with 10% neutral-buffered formalin for 30 min at 4°C and rinsed in PBS. Portions of the fixed gels were blocked with 5% FBS and permeabilized with 1% Triton X-100. Vinculin localization was examined by staining with the anti-vinculin antibody (10 μg/ml) and secondary detection was performed with the anti-mouse FITC-labeled antibody (10 μg/ml). Aggrecanase activity was detected with antiserum against the aggrecan-NITEGE neoepitope (10 μg/ml) and anti-rabbit AF488-conjugated antibody. The F-actin cytoskeleton was visualized by staining with AF594-phalloidin, and DNA was labeled with Hoechst dye. Cell viability and morphology were also assayed by staining with calcein AM and ethidium homodimer from the Live/Dead kit. The agarose gels were imaged with a Zeiss 510 laser scanning confocal microscope (Zeiss, Heidelberg, Germany). Fluorescence images of the F-actin cytoskeleton or calcein AM stain at 10× magnification were analyzed with Scion Image software (Frederick, MD). The area (A) and perimeter (P) for an individual cell were used to calculate the circularity (circularity $= 4\pi A/P^2$) as a quantitative measure of cell spreading, with a lower circularity indicating a greater degree of spreading (Fig. 1B, inset). At this magnification, each field contained approximately 200 cells, and circularities were calculated for all cells in a given field. Sensitivity analyses in preliminary experiments indicated that 50 cells per field were required for a representative population, and although similar trends could be observed using a 40× objective, the 10× magnification was selected to provide a sufficient sample size in each field. Circularity measurements were consistent across all experiments indicating that this technique is a

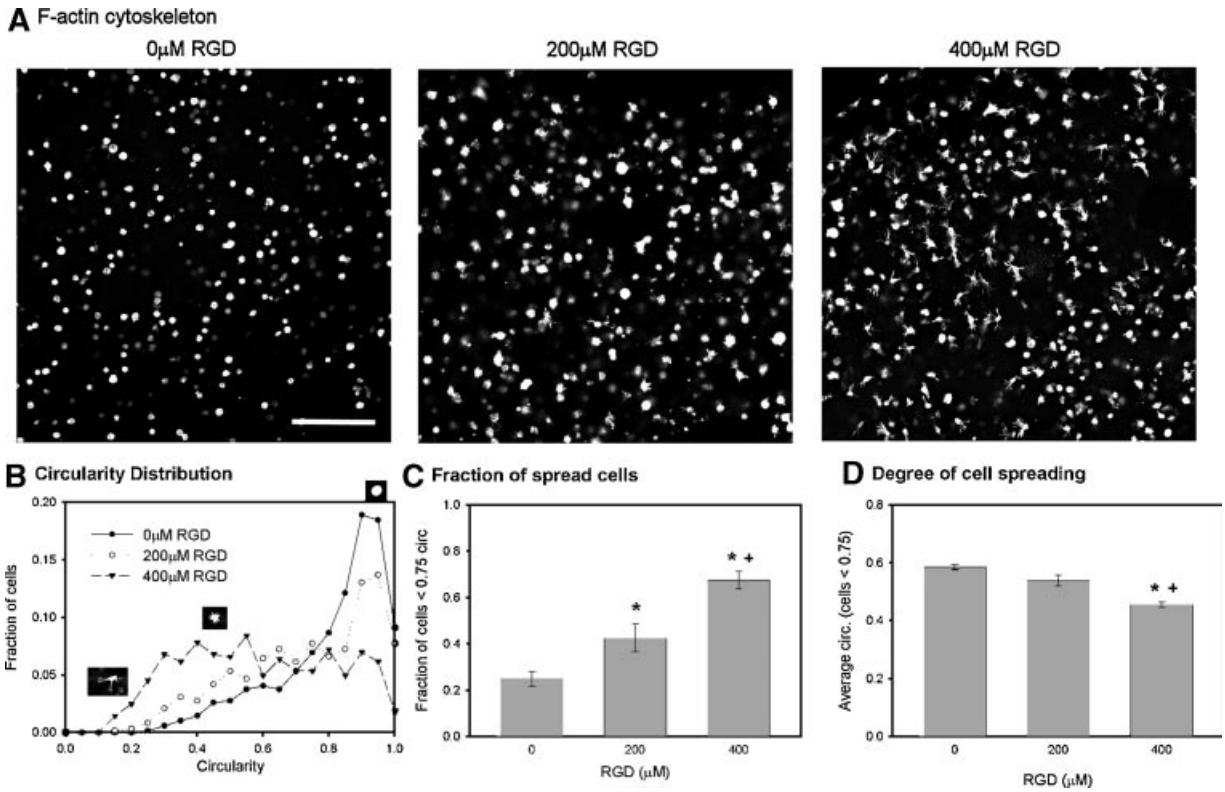

Fig. 1. Quantification of 3D BMSC morphology. BMSCs were seeded in agarose gels modified with 0, 200, or 400 μM RGD. Gels were cultured overnight in chondrogenic medium and stained with AlexaFluor594-phalloidin. A: Fluorescence images of the F-actin cytoskeleton were taken with a confocal microscope (10× magnification, scale bar = 200μm). B: The distribution of cell circularities from 3 random fields was plotted for each RGD density (insets showing representative cell morphologies), and (C) the fraction of spread cells was calculated for each field as the fraction with circularities less than 0.75. D: The degree of spreading was measured by the average circularity of the spread cells (<0.75 circ). n = 3 fields/density, $^{*}P < 0.05$ versus 0 μM, $^{+}P < 0.05$ versus 200 μM.

robust and quantitative tool for measuring cell morphology in a 3D environment.

Biochemical assays

The agarose gel constructs were weighed wet, lyophilized, and sequentially digested with Proteinase K (1 mg/80 mg sample) at 60°C overnight and agarase (4 U/construct) at 45°C for 4 h. The sulfated glycosaminoglycan (sGAG) contents were measured using the 1,9-dimethylmethylene blue assay (Farndale et al., 1982), and the DNA contents were measured using the Hoechst dye assay (Kim et al., 1988). Media samples were also analyzed for sGAG content using the DMMB assay and for mitochondrial activity using the WST-1 assay according to the manufacturer's instructions. To measure alkaline phosphatase activity, gels were rinsed in PBS for 20 min, immersed in 1% Triton X-100, and snap frozen to lyse the cells. The agarose gels were homogenized and centrifuged at 1,200*g*. The lysate was then removed and analyzed for alkaline phosphatase activity by measuring colorimetric reaction with the alkaline phosphatase substrate p-nitrophenyl phosphate.

Real-time RT-PCR

RNA was isolated from the agarose gels using the Tri-spin method (Chomczynski and Sacchi, 1987). Gels were immediately dissociated in lysis buffer containing 2-mercaptoethanol. RNA was extracted from the gel using the Trizol reagent and chloroform and precipitated with 100% isoproponol. The RNA was further purified using the Qiagen RNeasy kit according to the manufacturer's protocol. Total RNA (1 μg) was reverse transcribed to cDNA using the Promega AMV reverse transcriptase kit. Gene expression was measured by real-time RT-PCR using the SybrGreen master mix and custom primers for bovine collagen II (Brodkin et al., 2004), aggrecan (Brodkin et al., 2004), collagen I (Brodkin et al., 2004), and osteocalcin (Bosnakovski et al., 2005). The PCR reactions and detection were performed with an ABI Prism 7700 (Applied Biosystems, Forest City, CA).

Data analysis

All data are presented as the mean ± SEM. The fractions of spread cells were transformed using an arcsine function, and gene expression levels were transformed by a Box-Cox transformation for normality (Sokal and Rohlf, 1994). Data were analyzed by a two factor general linear model with RGD density/gel type and media conditions as factors. Dunnet's test was used to compare treatments with the blocking antibodies to the isotype control. All other pairwise comparisons were performed with Tukey's test. Significance was at $P < 0.05$.

Results

RGD-modified agarose gels promote quantifiable changes in 3D cell morphology

BMSCs were seeded into 3% agarose gels modified with 0, 200, or 400 μM final densities of the RGD peptide. After 24 h in

chondrogenic medium, cell spreading could be observed in the RGD-modified gels by fluorescence staining of the F-actin cytoskeleton and confocal microscopy (Fig. 1A). BMSCs displayed distinct cytoskeletal projections, and there were more spread cells within the 400 μM gels than the 200 μM gels. Changes in BMSC morphology were quantified by analyzing three randomly selected 10× images for each RGD density and calculating the circularity of all cells. The distribution of circularities in the unmodified gels displayed a large peak at 0.9 (Fig. 1B), indicative of highly rounded cells (circularity = 1 for a perfect circle). The size of this peak decreased with increasing RGD density, and the circularity distribution shifted towards lower circularities, characteristic of greater cell spreading. The fraction of cells with circularities less than 0.75 (below the major peak in 0 μM gels) was calculated for each field. RGD peptide significantly increased the fraction of spread cells in a density dependent manner (Fig. 1C). Furthermore, the 400 μM RGD density significantly reduced the average circularity of the spread cells compared to the 0 and 200 μM densities (Fig. 1D), indicating that interactions with the peptide also increased the degree of cell spreading. These results demonstrate that RGD-modified agarose gels promote RGD density-dependent changes in BMSC morphology.

3D cell spreading involves integrin-mediated adhesion

Integrin-mediated spreading in RGD-modified agarose was examined by immunofluorescence detection of vinculin and functional blocking with integrin-specific antibodies. BMSCs in the RGD-modified gels displayed large projections of the F-actin cytoskeleton that co-localized with vinculin, while cells in the RGE-modified gels remained rounded and had lower levels of localized vinculin staining (Fig. 2A). Blocking with the anti-αvβ3 antibody significantly reduced cell spreading, while blocking with the anti-β1 antibody significantly increased spreading (Fig. 2B). Together, these results suggest that the observed changes in cytoskeletal organization were associated with integrin-mediated adhesion involving at least the αvβ3 receptor and vinculin recruitment.

Cell spreading could also be inhibited with 10 μM Y-27632, which inhibits ROCK activity, or with 0.3 μM cytochalasin D, which prevents actin polymerization. These doses were selected based on preliminary dose-response experiments and represent the minimum amount required to significantly reduce 3D cell spreading (not shown). Treatment with Y-27632 or cytochalasin D at these levels did not appear to affect cell viability after 24 h (Fig. 2C) or mitochondrial activity after 6 days (Fig. 2C). These doses of the inhibitors significantly reduced cell

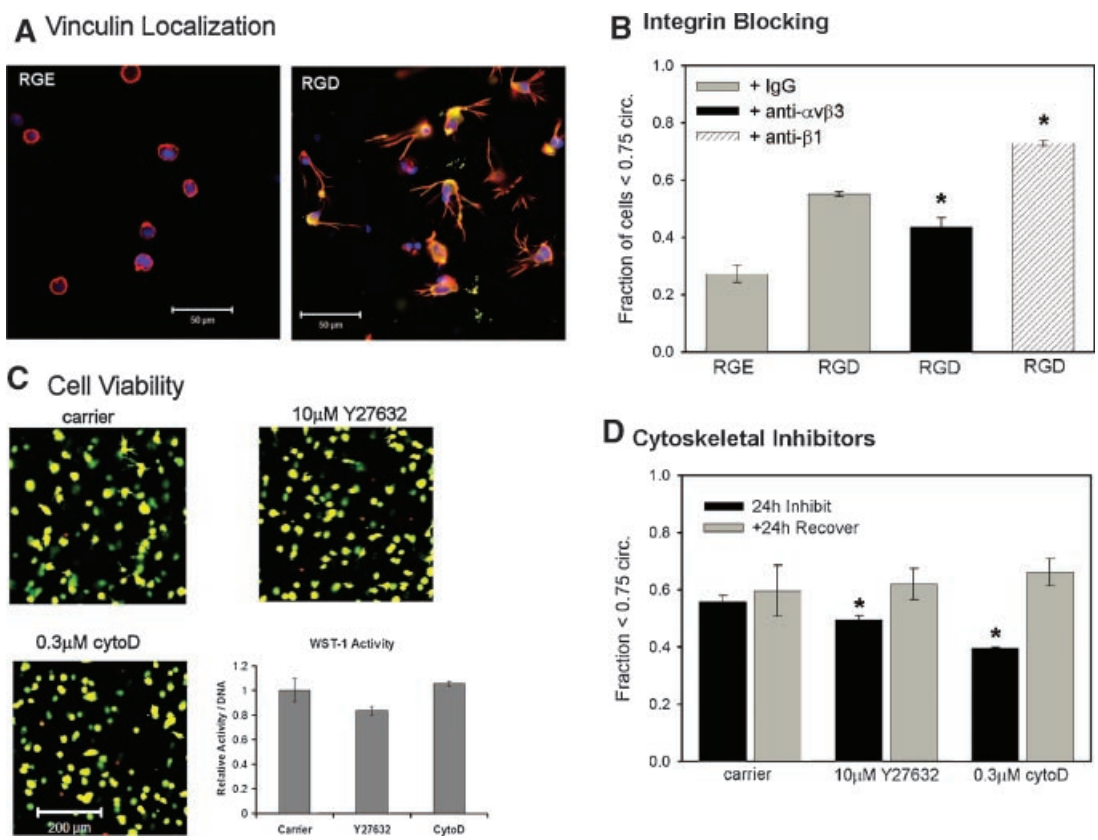

Fig. 2. Integrin dependent spreading and cytoskeletal organization. A: Vinculin localization (green) and the F-actin cytoskeleton (red) were examined by confocal microscopy (blue = DNA) 24 h after seeding BMSCs in 400 μM RGE or RGD modified gels. B: Specific integrin receptors were blocked with 20 μg/ml of anti-β1 or anti-αvβ3 antibodies prior to seeding BMSCs into 200 μM RGE/RGD gels. Cell spreading was quantified by analyzing fluorescence images of the F-actin cytoskeleton. C: Inhibitor toxicity was evaluated by Live/Dead staining following a 24 h treatment with 10 μM Y-27632, 0.3 μM cytochalasin D (cytoD), or carrier (0.1% DMSO) and by measuring the mitochondrial activity after 6 days with the WST-1 assay, n = 4 gels/condition. (D) The influence of these inhibitors on cell spreading was measured by analyzing images of the calcein AM stain after 24 h of inhibitor treatment and again 24 h after removing the inhibitors. All experiments were in chondrogenic medium (10 ng/ml TGF-β1 and 100 nM dexamethasone). n = 3 fields/condition, *$P < 0.05$ versus IgG or carrier.

spreading in 200 μM RGD gels after 24 h (Fig. 2D). In addition, BMSCs were able to fully recover their spread morphology 24 h after removal of the inhibitors (Fig. 2D), verifying that there were no cytotoxic or sustained inhibitory effects of these compounds on BMSC activity.

Interactions with RGD-modified agarose inhibit BMSC chondrogenesis

To examine the effects of integrin-mediated adhesion to RGD on chondrogenesis within the agarose gel system, BMSCs were seeded into unmodified, 400 μM RGE-, or 400 μM RGD-modified gels and cultured for 7 days in basal or chondrogenic (10 ng/ml TGF-β1 and 100 nM dexamethasone) medium. At day 7, the DNA content was significantly higher in the chondrogenic groups with no differences among gel types (Fig. 3A). The chondrogenic medium also significantly stimulated sGAG production over the basal condition (Fig. 3B). There were no differences in sGAG accumulation between unmodified and RGE gels, but there was significantly less (24%) sGAG in the RGD-modified gels compared to the unmodified gels (Fig. 3B). These results provided initial evidence that interactions with the RGD-modified agarose inhibit the chondrogenic response of BMSCs to TGF-β1 and dexamethasone.

RGD density and cytoskeletal organization modulate sGAG accumulation and release during BMSC chondrogenesis

The influence of RGD density and cytoskeletal organization on BMSC chondrogenesis was investigated by seeding cells into agarose with varying densities of RGD peptide and culturing the gels in chondrogenic medium supplemented with Y-27632, cytochalasin D, or carrier (0.01% DMSO). RGD densities ranging from 0 to 400 μM were generated by varying the ratio of RGE to RGD while maintaining 400 μM of total peptide in all gels to account for any non-specific effects of the synthetic peptides on BMSC differentiation. Analysis of the F-actin images at 24 h demonstrated that cell spreading increased with increasing RGD densities consistent with the previous experiments (Fig. 4A). Addition of 10 μM Y-27632 did not alter cell morphology, while 0.3 μM cytochalasin D completely blocked cell spreading in the 200 and 400 μM RGD gels. After 6 days in culture, RGD did not alter the DNA content within the gels, but treatment with Y-27632 decreased the DNA content in the 400 μM RGD gels only (Fig. 4B). RGD densities of 40, 200, and 400μM significantly inhibited sGAG accumulation in a dose-dependent manner (Fig. 4C). Treatment with Y-27632 decreased sGAG accumulation to similar levels for all RGD densities. Disruption of the F-actin cytoskeleton with cytochalasin D resulted in similar amounts of sGAG accumulation across all RGD densities, effectively lowering the sGAG contents in 0 and 4 μM gels and increasing the sGAG content in 400 μM gels as compared to vehicle treatment (Fig. 4C). These findings indicate that the density-dependent effects of RGD adhesion on BMSC chondrogenesis involve changes in the F-actin cytoskeleton.

BMSC morphology in the 0, 40, and 400 μM RGD gels was also examined after 6 days of culture with Y-27632 and cytochalasin D. Small cytoskeletal projections could be observed in the 0 μM gels by day 6 (Fig. 5A), and BMSCs in the 40 μM gels appeared to have larger projections and actin stress fibers (Fig. 5B). Cells in the 400 μM gels formed multi-cell clusters with clear actin stress fibers (Fig. 5C). Addition of Y-27632 did not influence cell morphology at any RGD density, while treatment with cytochalasin D promoted rounded morphologies at each density and no cell aggregation in the 400 μM gels (Fig. 5A–C). Given the similar levels of DNA across RGD densities, it is evident that RGD adhesion promotes cell migration and aggregate formation within the agarose gels, and this process requires organization of the F-actin cytoskeleton.

In contrast to the effects on sGAG accumulation, the cumulative sGAG released to the media was significantly higher for the 400 μM RGD gels than for the 0 μM gels (Fig. 4D). Addition of Y-27632 inhibited sGAG release into the media at all RGD densities, and cytochalasin D significantly reduced sGAG release at the 0 and 400 μM densities only. The levels of sGAG released to the media were small compared to those retained within the gels, and the total sGAG production (media plus gel, not shown) displayed the same trends as the sGAG accumulation data. Immunofluorescence detection of the NITEGE neoepitope revealed higher levels of aggrecanase-mediated aggrecan degradation in the 400 μM RGD gels (Fig. 5D). The NITEGE signal was localized within the multi-cell aggregates and in the extracellular space, and treatment with cytochalasin blocked NITEGE generation. Taken together, these results suggest that adhesion and cell spreading on RGD promote a catabolic release of sGAG that is in part mediated by aggrecanase-specific cleavage of the aggrecan core protein.

RGD adhesion differentially regulates BMSC activity in chondrogenic and serum-supplemented medium

To investigate the specificity of RGD interactions on chondrogenesis, BMSCs were seeded into 200 μM RGE or

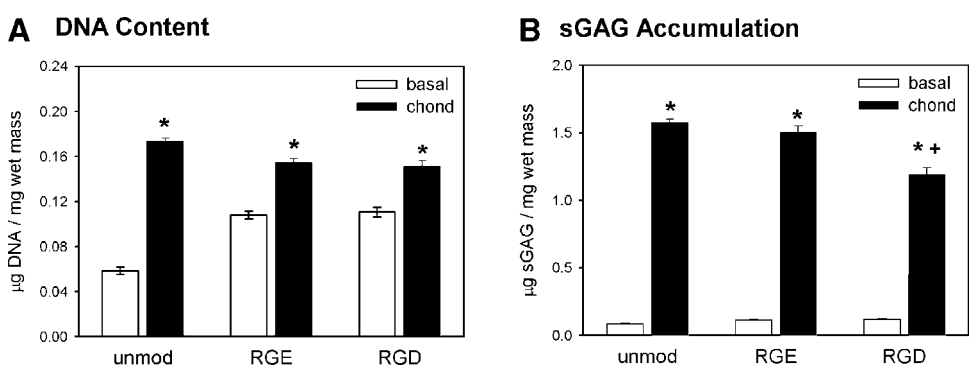

Fig. 3. Effects of RGD adhesion on chondrogenesis. BMSCs were seeded into unmodified, 400 μM RGE, or 400 μM RGD gels and cultured for 7 days in basal or chondrogenic medium. A: The DNA contents within the gels were measured using the Hoechst dye assay, and (B) the levels of sGAG accumulation were measured with the DMMB assay. n = 6 gels/condition, $^{*}P < 0.05$ versus basal medium, $^{+}P < 0.05$ versus RGE gels.

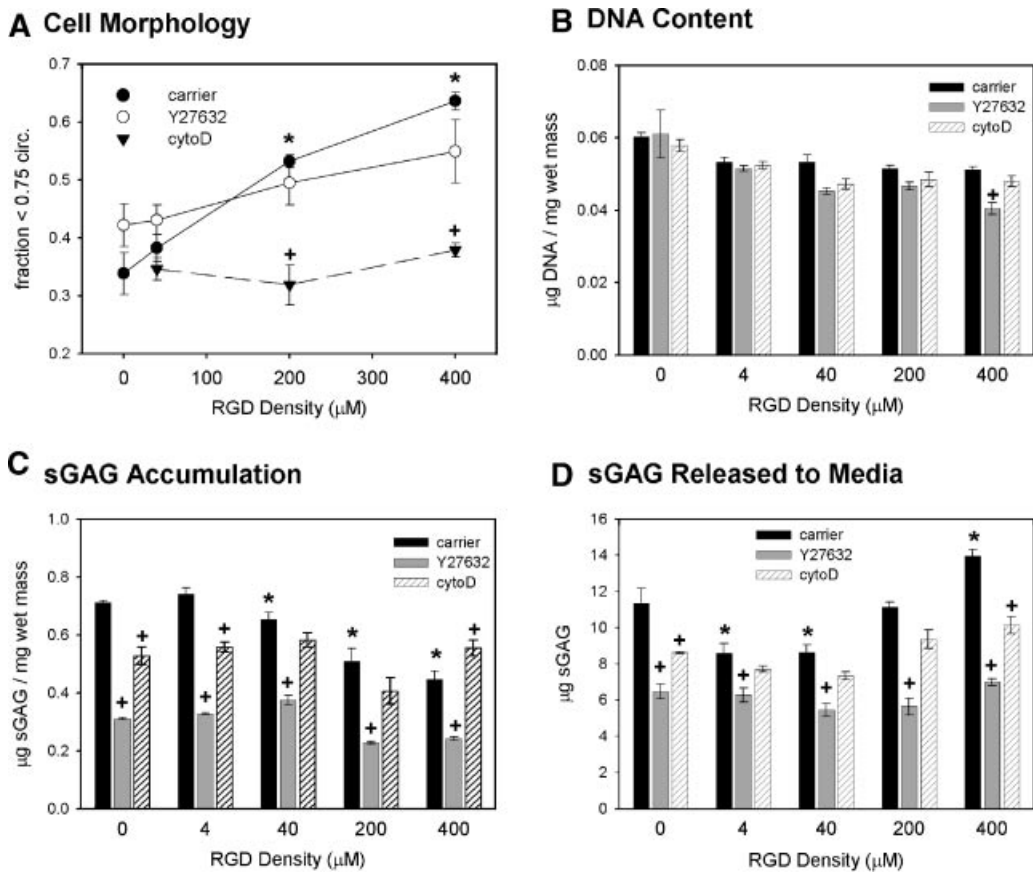

Fig. 4. Influence of RGD density and cytoskeletal integrity on chondrogenesis. BMSCs were seeded into modified agarose gels with 0, 4, 40, 200, and 400 μM densities of RGD and cultured up to 6 days in chondrogenic medium supplemented with carrier (0.01% DMSO), 10 μM Y-27632, or 0.3 μM cytochalasin D (cytoD). A: Cell morphology was measured by analyzing fluorescence images of the F-actin cytoskeleton 24 h after seeding. n = 3 fields/condition (B) The DNA content was measured using the Hoechst dye assay. C: The sGAG accumulation within the gels and (D) cumulative sGAG released to the media were measured by the DMMB assay. n = 4 gels/condition, $^{*}P < 0.05$ versus 0 μM, $^{+}P < 0.05$ versus carrier at same RGD density.

RGD-modified gels and cultured for 8 days in chondrogenic or 10% FBS supplemented medium. The mRNA levels of chondrogenic and osteogenic genes were measured by real-time RT-PCR. In the RGE gels, BMSCs cultured with the chondrogenic medium expressed significantly higher levels of collagen II and aggrecan mRNA transcripts than cells in the serum-supplemented medium, but BMSCs in the 10% FBS medium expressed significantly higher amounts of osteocalcin. In the presence of the chondrogenic medium, RGD interactions significantly inhibited chondrogenic gene expression but had no effect on osteocalcin gene expression. Conversely, RGD interactions had no effect on chondrogenic gene expression in serum-supplemented medium but significantly increased osteocalcin and collagen I expression. These distinct responses to RGD-modified agarose in chondrogenic and 10% FBS media suggest that RGD adhesion can differentially regulate the differentiation of BMSCs depending on the specific biochemical stimuli. While the markers examined do not definitively indicate osteogenic specific differentiation, the response to the serum-supplemented medium was characteristic of osteogenesis and consistent with previous findings (Shin et al., 2005).

The density dependent effects of RGD adhesion on the response of BMSCs to serum-supplemented medium were examined by seeding cells into 0, 4, and 200 μM RGD gels and measuring the alkaline phosphatase activity after 8 days of culture in 10% FBS medium. Similar to the previous experiment, RGD adhesion had no effect on the DNA content within the gels but significantly increased alkaline phosphatase activity in a dose-dependent manner. These results demonstrate that in addition to the effects on gene expression, RGD interactions enhance alkaline phosphatase activity, characteristic of increased osteogenic differentiation, and BMSCs display opposite density dependent responses to RGD when exposed to different biochemical stimuli.

Discussion

The goal of this study was to examine the interactions between integrin ligand density and cytoskeletal organization in regulating the chondrogenesis of mesenchymal progenitor cells. For this investigation, agarose hydrogels were modified with synthetic RGD peptides to present controlled densities of cell adhesive ligands within a three-dimensional culture environment. The agarose system was chosen because it is a well characterized material for culturing chondrocytes (Benya and Shaffer, 1982; Kolettas et al., 1995; Mouw et al., 2005) and chondro-progenitors (Mauck et al., 2006) and provides a non-adhesive background for tethering various proteins and peptides (Dodla and Bellamkonda, 2006). In these studies, integrin-mediated adhesion to the RGD peptide promoted

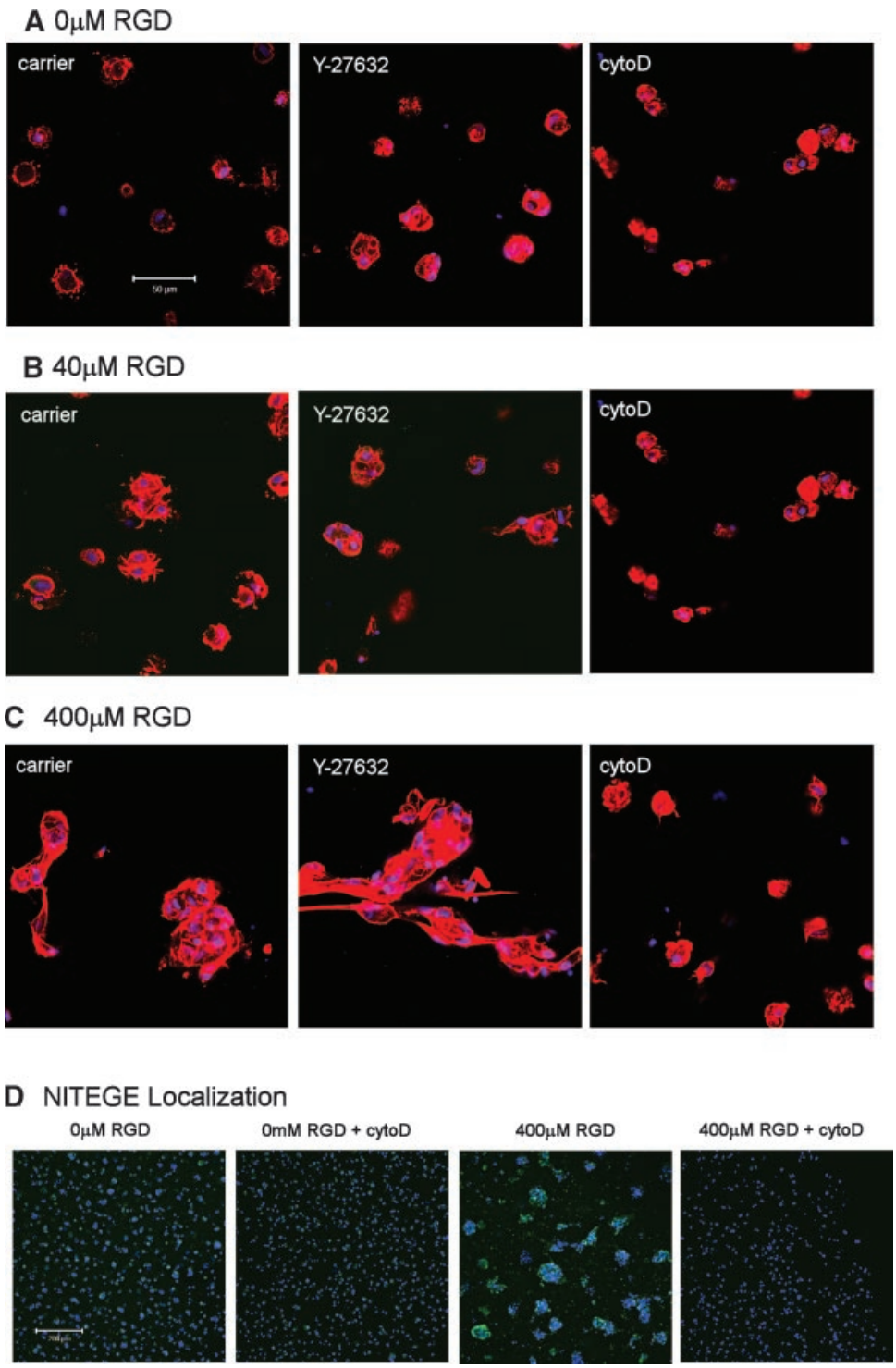

Fig. 5. Cellular morphology and NITEGE localization in long-term cultures. Cell morphology was examined after 6 days in (A) 0, (B) 40, and (C) 400 μM RGD gels cultured with the carrier, Y-27632, or cytochalasin D (cytoD) (red = F-actin, blue = DNA). D: Aggrecanase activity was detected by immunostaining with antiserum against the aggrecan-NITEGE neoepitope (green = NITEGE, blue = DNA).

quantifiable and density-dependent increases in BMSC spreading, and interactions with the RGD-modified gels inhibited the chondrogenic response to TGF-β1 and dexamethasone concomitant with the changes in cell morphology. Disruption of F-actin polymerization with cytochalasin D blocked BMSC spreading and prevented the inhibitory effects of RGD adhesion on sGAG production. Interestingly, interactions with the RGD-modified agarose also appeared to facilitate cell migration and aggregation within the gel and promoted the catabolic release of sGAG to the media.

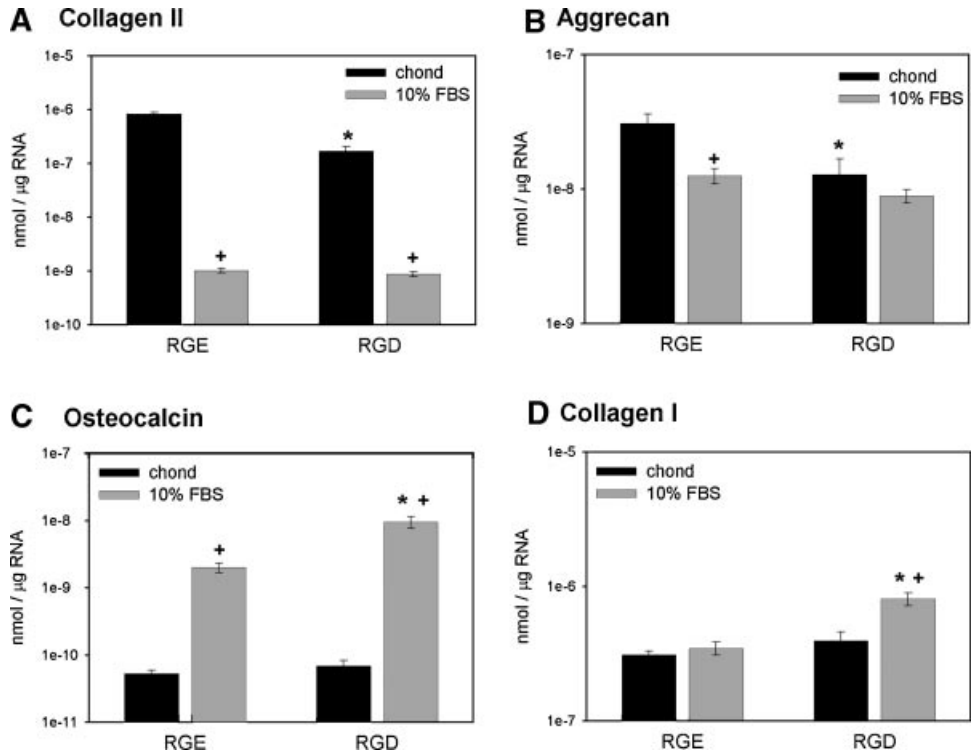

Fig. 6. Influence of RGD adhesion and culture conditions on mRNA expression. BMSCs in 200 μM RGE or RGD gels were cultured for 8 days in chondrogenic (10 ng/ml TGF-β1 and 100 nM dexamethasone) or 10% serum-supplemented medium. Expression of the chondrogenic genes, (A) collagen type II and (B) aggrecan, and the osteogenic genes, (C) osteocalcin and (D) collagen type I, were measured by real-time RT-PCR. n = 4/condition, $^{*}P < 0.05$ versus RGE gels, $^{+}P < 0.05$ versus chondrogenic medium.

The examination of alternative lineage markers suggests that these responses were specific to chondrogenic differentiation and that RGD adhesion may differentially regulate BMSC osteogenesis, depending on the biochemical context. Overall, these findings provide new insights into the role of cell morphology in the regulation of chondrogenesis and demonstrate the ability of coordinated signals from growth factors and the ECM to promote differentiation along specific mesenchymal lineages.

Previous studies have reported varying roles for the F-actin cytoskeleton in the process of chondrogenesis. For example, disruption of actin polymerization with cytochalasin D enhanced the chondrogenesis of chick limb bud cells in monolayer (Lim et al., 2000), but the addition of Y-27632 and cytochalasin to micromass cultures inhibited chondrocytic gene expression (Woods et al., 2005). The results of the current study suggest that the degree of cytoskeletal organization may be an important regulator of differentiation. For the rounded cells in 0 μM RGD gels, disruption of the F-actin cytoskeleton inhibited the chondrocytic phenotype, but for cells in 400 μM RGD-modified agarose, blocking cell spreading actually increased sGAG production. These findings provide a potential explanation for the different responses observed in monolayer and micromass cultures and indicate that a minimal level of cytoskeletal organization may be required for optimal chondrogenesis and maintenance of the chondrocytic phenotype.

In the present study, the ROCK inhibitor Y-27632 significantly reduced sGAG production to similar levels at all RGD densities. In addition, the influences of Y-27632 on differentiation occurred without significantly altering cell morphology at the doses examined, and the inhibitor appeared to have no effect on BMSC aggregation in the 400 μM gels. Although ROCK is known to influence cytoskeletal organization by promoting actin-myosin contractility (Amano et al., 1996; Leung et al., 1996), one of its targets, myosin light chain (MLC), can also be phosphorylated by myosin light chain kinase (MLCK) (Totsukawa et al., 2000). Therefore, the formation of cytoskeletal projections and cell aggregation observed within the modified agarose gels may involve actin-myosin contractility independent of ROCK activity. Despite having little effect on cell morphology, the significant inhibition of sGAG production suggests that ROCK signaling interacts with other regulatory pathways. This result is consistent with a previous study in which constitutively active ROCK stimulated osteogenesis independently of changes in cell shape (McBeath et al., 2004). Furthermore, blocking RhoA signaling has been shown to inhibit TGF-β induced Smad2/3 phosphorylation in smooth muscle cells (Chen et al., 2006). Together, these reports provide additional evidence that ROCK regulates differentiation downstream of cytoskeletal organization.

The use of pharmacological inhibitors is limited by the potential for cytotoxic or non-specific effects on cellular activities. Doses of 10 μM Y-27632 and 0.3 μM cytochalasin D did not have noticeable effects on cell viability or the DNA content at low RGD densities. In addition, BMSCs were able to recover their spread morphologies within 24 h following inhibitor removal, suggesting that these doses did not have a toxic effect on cell function. It is possible that the inhibitors had non-specific effects on other signaling molecules or kinases that influence chondrogenesis; however, other investigations have reported similar effects on cell activity using both 10 μM

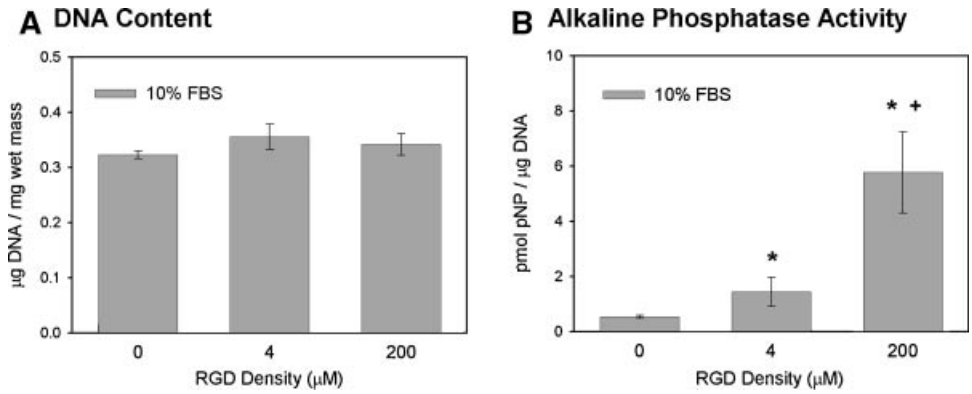

Fig. 7. RGD density dependent effects on alkaline phosphatase activity. BMSCs were seeded into 0, 4, or 200 μM RGD-modified agarose gels and cultured for 8 days in 10% FBS supplemented medium. A: The DNA content was measured by the Hoechst dye assay, and (B) alkaline phosphatase activity was measured by production of p-nitrophenyl (pNP) from the Sigma 104 phosphatase substrate. n = 6/condition, $^{*}P < 0.05$ with 0 μM, $^{+}P < 0.05$ with 4 μM.

Y-27632 and dominant negative RhoA (McBeath et al., 2004; Chen et al., 2006). Although there are no current indications of toxicity or non-specific effects on BMSC differentiation, genetic strategies for perturbing ROCK signaling and cytoskeletal organization would help to strengthen the findings presented in this study.

Interactions between integrin adhesion and cytoskeletal organization are critical for the formation of focal complexes and signal transduction (Nobes and Hall, 1995). In this study, functional blocking of αvβ3 integrins inhibited 3D cell spreading, but blocking with the anti-β1 integrin antibody significantly increased cell spreading. These results suggest that both receptors compete for the RGD ligand, but the αvβ3 integrin appears to be specifically involved in cell spreading and cytoskeletal organization, consistent with previous reports (Keselowsky et al., 2005). In this manner, αvβ3 integrin adhesion within the modified agarose system may regulate chondrogenesis through changes in cell morphology. However, cytoskeletal organization also provides feedback to integrin signaling by stabilizing the formation of focal complexes and recruiting signaling molecules such as FAK, ILK, and src (Amano et al., 2001; Galbraith et al., 2002; Gallant et al., 2005). Therefore, disrupting F-actin polymerization with cytochalasin D may have prevented signaling from the normal cell–matrix interactions that are important for chondrogenesis at low RGD densities, as well as the inhibitory effects of RGD adhesion at the higher densities. While the findings in the present study demonstrate a clear role for the F-actin cytoskeleton in mediating the response of BMSCs to the RGD-modified gels, it has yet to be established whether changes in cell morphology directly regulate chondrogenesis or whether cytoskeletal organization simply facilitates signaling through integrins and focal adhesion proteins.

In addition to cell spreading, RGD adhesion promoted cell aggregation within the agarose hydrogels and stimulated the catabolic release of sGAG to the media. These responses are consistent with TGF-β1 stimulation of cell migration during processes such as wound healing (Reynolds et al., 2005) and tumor cell invasion (Janji et al., 1999; Muraoka et al., 2002). Cell migration is known to involve the αvβ3 integrin receptor (Bayless et al., 2000; Reynolds et al., 2005) and is associated with increased proteolytic activity (Held-Feindt et al., 2006; Zaman et al., 2006). Similarly, the changes in chondrocyte morphology that occur during chondrocyte dedifferentiation have been implicated in interleukin-1 production and an inflammatory phenotype that promotes aggrecanase-mediated catabolism of proteoglycans (Kim et al., 2003). The results of the current study support these observations and further demonstrate that integrin adhesion to the ECM can induce aggrecanase-mediated degradation of proteoglycans.

The process of chondrogenesis is tightly regulated by many signals from the surrounding microenvironment. The present study demonstrates that cell–ECM interactions play a key role in mediating cues from the biochemical environment. Although interactions with the RGD-modified agarose inhibited the chondrogenic response to TGF-β1 and dexamethasone, the same cell–scaffold interactions enhanced the osteogenic response to serum-supplemented medium. These distinct responses of BMSCs to RGD-modified agarose suggest that coordination of signals from growth factors and the ECM provides a strategy for directing the lineage-specific differentiation of mesenchymal progenitors.

In addition to furthering the current understanding of mesenchymal progenitor cell differentiation, these findings may have important implications for the use of BMSCs or other progenitors in cell-based therapies and tissue-engineering. The development of appropriate biomaterials, as well as the optimization of cell culture conditions, will be essential for controlling cell fate within a tissue engineered construct. While cell adhesion to RGD-modified materials may be advantageous for enhancing bone regeneration, other cell–matrix interactions, such as collagen or proteoglycan interactions, may improve the in vitro chondrogenesis of BMSCs. Therefore, a greater understanding of the cell–matrix interactions involved in chondrogenesis will help direct the development of more sophisticated materials for cartilage repair and the application of mesenchymal progenitors in regenerative therapies.

Acknowledgments

This work was supported primarily by funding from the Georgia Tech/Emory Center (GTEC) for the Engineering of Living Tissues, an ERC Program of the National Science Foundation under Award Number EEC-9731643.

Literature Cited

Ai S, Kuzuya M, Koike T, Asai T, Kanda S, Maeda K, Shibata T, Iguchi A. 2001. Rho-Rho kinase is involved in smooth muscle cell migration through myosin light chain phosphorylation-dependent and independent pathways. Atherosclerosis 155:321–327.

Amano M, Ito M, Kimura K, Fukata Y, Chihara K, Nakano T, Matsuura Y, Kaibuchi K. 1996. Phosphorylation and activation of myosin by Rho-associated kinase (Rho-kinase). J Biol Chem 271:20246–20249.
Amano T, Tanabe K, Eto T, Narumiya S, Mizuno K. 2001. LIM-kinase 2 induces formation of stress fibres, focal adhesions and membrane blebs, dependent on its activation by Rho-associated kinase-catalysed phosphorylation at threonine-505. Biochem J 354:149–159.
Bayless KJ, Salazar R, Davis GE. 2000. RGD-dependent vacuolation and lumen formation observed during endothelial cell morphogenesis in three-dimensional fibrin matrices involves the alpha(v)beta(3) and alpha(5)beta(1) integrins. Am J Pathol 156:1673–1683.
Benya PD, Shaffer JD. 1982. Dedifferentiated chondrocytes reexpress the differentiated collagen phenotype when cultured in agarose gels. Cell 30:215–224.
Bosnakovski D, Mizuno M, Kim G, Takagi S, Okumura M, Fujinaga T. 2005. Isolation and multilineage differentiation of bovine bone marrow mesenchymal stem cells. Cell Tissue Res 319:243–253.
Brodkin KR, Garcia AJ, Levenston ME. 2004. Chondrocyte phenotypes on different extracellular matrix monolayers. Biomaterials 25:5929–5938.
Calderwood DA, Zent R, Grant R, Rees DJ, Hynes RO, Ginsberg MH. 1999. The Talin head domain binds to integrin beta subunit cytoplasmic tails and regulates integrin activation. J Biol Chem 274:28071–28074.
Chen S, Crawford M, Day RM, Briones VR, Leader JE, Jose PA, Lechleider RJ. 2006. RhoA modulates Smad signaling during transforming growth factor-beta-induced smooth muscle differentiation. J Biol Chem 281:1765–1770.
Chomczynski P, Sacchi N. 1987. Single-step method of RNA isolation by acid guanidinium thiocyanate-phenol-chloroform extraction. Anal Biochem 162:156–159.
Connelly JT, Garcia AJ, Levenston ME. 2007. Inhibition of in vitro chondrogenesis in RGD-modified three-dimensional alginate gels. Biomaterials 28:1071–1083.
Critchley DR. 2004. Cytoskeletal proteins talin and vinculin in integrin-mediated adhesion. Biochem Soc Trans 32:831–836.
Dodla MC, Bellamkonda RV. 2006. Anisotropic scaffolds facilitate enhanced neurite extension in vitro. J Biomed Mater Res A 78:213–221.
Farndale RW, Sayers CA, Barrett AJ. 1982. A direct spectrophotometric microassay for sulfated glycosaminoglycans in cartilage cultures. Connect Tissue Res 9:247–248.
Galbraith CG, Yamada KM, Sheetz MP. 2002. The relationship between force and focal complex development. J Cell Biol 159:695–705.
Gallant ND, Michael KE, Garcia AJ. 2005. Cell adhesion strengthening: Contributions of adhesive area, integrin binding, and focal adhesion assembly. Mol Biol Cell 16:4329–4340.
Giancotti FG, Ruoslahti E. 1999. Integrin signaling. Science 285:1028–1032.
Held-Feindt J, Paredes EB, Blomer U, Seidenbecher C, Stark AM, Mehdorn HM, Mentlein R. 2006. Matrix-degrading proteases ADAMTS4 and ADAMTS5 (disintegrins and metalloproteinases with thrombospondin motifs 4 and 5) are expressed in human glioblastomas. Int J Cancer 118:55–61.
Imamura F, Mukai M, Ayaki M, Akedo H. 2000. Y-27632, an inhibitor of rho-associated protein kinase, suppresses tumor cell invasion via regulation of focal adhesion and focal adhesion kinase. Jpn J Cancer Res 91:811–816.
Iwamoto H, Nakamuta M, Tada S, Sugimoto R, Enjoji M, Nawata H. 2000. A p160ROCK-specific inhibitor, Y-27632, attenuates rat hepatic stellate cell growth. J Hepatol 32:762–770.
Janji B, Melchior C, Gouon V, Vallar L, Kieffer N. 1999. Autocrine TGF-beta-regulated expression of adhesion receptors and integrin-linked kinase in HT-144 melanoma cells correlates with their metastatic phenotype. Int J Cancer 83:255–262.
Kaartinen V, Haataja L, Nagy A, Heisterkamp N, Groffen J. 2002. TGFbeta3-induced activation of RhoA/Rho-kinase pathway is necessary but not sufficient for epithelio-mesenchymal transdifferentiation: Implications for palatogenesis. Int J Mol Med 9:563–570.
Keselowsky BG, Collard DM, Garcia AJ. 2005. Integrin binding specificity regulates biomaterial surface chemistry effects on cell differentiation. Proc Natl Acad Sci USA 102:5953–5957.
Kim YJ, Sah RL, Doong JY, Grodzinsky AJ. 1988. Fluorometric assay of DNA in cartilage explants using Hoechst 33258. Anal Biochem 174:168–176.
Kim SJ, Hwang SG, Kim IC, Chun JS. 2003. Actin cytoskeletal architecture regulates nitric oxide-induced apoptosis, dedifferentiation, and cyclooxygenase-2 expression in articular chondrocytes via mitogen-activated protein kinase and protein kinase C pathways. J Biol Chem 278:42448–42456.
Kolettas E, Buluwela L, Bayliss MT, Muir HI. 1995. Expression of cartilage-specific molecules is retained on long-term culture of human articular chondrocytes. J Cell Sci 108:1991–1999.
Leung T, Chen XQ, Manser E, Lim L. 1996. The p160 RhoA-binding kinase ROK alpha is a member of a kinase family and is involved in the reorganization of the cytoskeleton. Mol Cell Biol 16:5313–5327.
Lim YB, Kang SS, Park TK, Lee YS, Chun JS, Sonn JK. 2000. Disruption of actin cytoskeleton induces chondrogenesis of mesenchymal cells by activating protein kinase C-alpha signaling. Biochem Biophys Res Commun 273:609–613.
Maheshwari G, Brown G, Lauffenburger DA, Wells A, Griffith LG. 2000. Cell adhesion and motility depend on nanoscale RGD clustering. J Cell Sci 113:1677–1686.
Mauck RL, Yuan X, Tuan RS. 2006. Chondrogenic differentiation and functional maturation of bovine mesenchymal stem cells in long-term agarose culture. Osteoarthritis Cartilage 14:179–189.
McBeath R, Pirone DM, Nelson CM, Bhadriraju K, Chen CS. 2004. Cell shape, cytoskeletal tension, and RhoA regulate stem cell lineage commitment. Dev Cell 6:483–495.
Mouw JK, Case ND, Guldberg RE, Plaas AH, Levenston ME. 2005. Variations in matrix composition and GAG fine structure among scaffolds for cartilage tissue engineering. Osteoarthritis Cartilage 13:828–836.
Muraoka RS, Dumont N, Ritter CA, Dugger TC, Brantley DM, Chen J, Easterly E, Roebuck LR, Ryan S, Gotwals PJ, Koteliansky V, Arteaga CL. 2002. Blockade of TGF-beta inhibits mammary tumor cell viability, migration, and metastases. J Clin Invest 109:1551–1559.
Newman P, Watt FM. 1988. Influence of cytochalasin D-induced changes in cell shape on proteoglycan synthesis by cultured articular chondrocytes. Exp Cell Res 178:199–210.
Nobes CD, Hall A. 1995. Rho, rac, and cdc42 GTPases regulate the assembly of multimolecular focal complexes associated with actin stress fibers, lamellipodia, and filopodia. Cell 81:53–62.
Reynolds LE, Conti FJ, Lucas M, Grose R, Robinson S, Stone M, Saunders G, Dickson C, Hynes RO, Lacy-Hulbert A, Hodivala-Dilke K. 2005. Accelerated re-epithelialization in beta3-integrin-deficient-mice is associated with enhanced TGF-beta1 signaling. Nat Med 11:167–174.
Shin H, Temenoff JS, Bowden GC, Zygourakis K, Farach-Carson MC, Yaszemski MJ, Mikos AG. 2005. Osteogenic differentiation of rat bone marrow stromal cells cultured on Arg-Gly-Asp modified hydrogels without dexamethasone and beta-glycerol phosphate. Biomaterials 26:3645–3654.
Sokal RR, Rohlf FJ. 1994. Biometry: W.H. Freeman.
Totsukawa G, Yamakita Y, Yamashiro S, Hartshorne DJ, Sasaki Y, Matsumura F. 2000. Distinct roles of ROCK (Rho-kinase) and MLCK in spatial regulation of MLC phosphorylation for assembly of stress fibers and focal adhesions in 3T3 fibroblasts. J Cell Biol 150:797–806.
von der Mark K, Gauss V, von der Mark H, Muller P. 1977. Relationship between cell shape and type of collagen synthesised as chondrocytes lose their cartilage phenotype in culture. Nature 267:531–532.
Woods A, Beier F. 2006. RhoA/ROCK signaling regulates chondrogenesis in a context-dependent manner. J Biol Chem 281:13134–13140.
Woods A, Wang G, Beier F. 2005. RhoA/ROCK signaling regulates Sox9 expression and actin organization during chondrogenesis. J Biol Chem 280:11626–11634.
Zaman MH, Trapani LM, Sieminski AL, Mackellar D, Gong H, Kamm RD, Wells A, Lauffenburger DA, Matsudaira P. 2006. Migration of tumor cells in 3D matrices is governed by matrix stiffness along with cell-matrix adhesion and proteolysis. Proc Natl Acad Sci USA 103:10889–10894.